Journal of Applied Electrochemistry **32**: 921–927, 2002.

Defect dimension evaluation in organic coated galvanized steel by electrochemical impedance spectroscopy☆

F. DEFLORIAN[1,*], L. FEDRIZZI[2], S. ROSSI[1] and P.L. BONORA[1]
[1]*Department of Materials Engineering, University of Trento, Italy*
[2]*Department ICMMPM, University of Rome "La Sapienza", Rome, Italy*
*(*author for correspondence)*

Received 22 June 2001; accepted in revised form 16 April 2002

Key words: defects, electrochemical impedance spectroscopy, galvanized steel, organic coatings

Abstract

The protective effectiveness of organic coatings, in controlling corrosion processes by the barrier effect, is dominated by the absence of defects passing through the coating and reaching the substrate. It is, however, difficult in general to identify and quantify the presence of defects. This work is an effort to reach a more precise quantification of the size of defect in organic coatings by means of electrochemical impedance spectroscopy (EIS) measurements. Artificial defects with controlled dimensions between 60 and 200 μm were produced on organic coated galvanized steel (coil coating). After optimization of the experimental procedure for EIS data acquisition, the parameters obtained, according to a classical electrical model, were correlated with the defect dimensions. The results show that the double layer capacitance (C_{dl}) values depend in linearly on the defects area, while this is not true for the pore resistance (R_p) values, as the electrolyte resistivity inside the defects is a function of the defect size. Further work is necessary to extend the results to smaller defects and different systems, that is, different organic coatings and substrates.

1. Introduction

The protective effectiveness of organic coatings controlling corrosion processes by the barrier effect is dominated by the absence of any defect (pores, scratches etc.) passing through the coating and reaching the substrate which can cause the initiation of corrosion [1, 2]. Such defects may be induced during coating deposition (pores, bubbles, areas with insufficient curing etc.) or in service (scratches, impacts, wear etc.) [3]. The identification of defects is often difficult because they are in general very small, but even more difficult is the quantification of the defect dimension. In general optical observations, including the use of optical microscopes, and electrical tests, checking the electrical conductivity of the coating when a high voltage is applied, are used [4].

For many years it has been known that the presence of defects can also be determined by EIS measurements [5–11]. We can distinguish in the total impedance the contribution due to the organic coating and therefore the ionic resistance of the coating. But ions can pass through the coating mainly if the coating is defective and therefore a low coating resistance means a higher presence of defects considering the coating thickness to be constant [7]. Similarly the electrochemical parameters related to the corrosion reaction (charge transfer resistance and double layer capacitance) can change due to variation of the wet or reactive area, and again therefore because of the presence or the development of defects [12].

We show, in Figure 1, the classical electrical model (equivalent electrical circuit) for an organic coating with a defect when an a.c. voltage is applied. An evident simplification in Figure 1 is the cylindrical shape of the defect although far from typical. However, we may consider this assumption generally acceptable.

The model in Figure 1 shows the correlation between electrical parameters and defect dimensions. First the pore resistance R_p. Defining ρ as the ion resistivity of the defect (i.e., electrolyte resistivity inside the defect), we can write the following equation relating the defect dimension to the measured pore resistance R_p:

$$R_p = \rho \frac{d}{A_p} \tag{1}$$

where d is the coating thickness and A_p the unknown defect area.

The double layer capacitance C_{dl} and the charge transfer resistance R_{ct} are also related to the uncovered metal surface by the following equations [13]:

$$R_{ct} = \frac{R_{ct}^{\circ}}{A_r} \tag{2}$$

$$C_{dl} = \frac{C_{dl}^{\circ}}{A_w} \tag{3}$$

☆This paper was initially presented at the 5th International Symposium on Electrochemical Impedance Spectroscopy at Marilleva, Trento, Italy, June 2001.

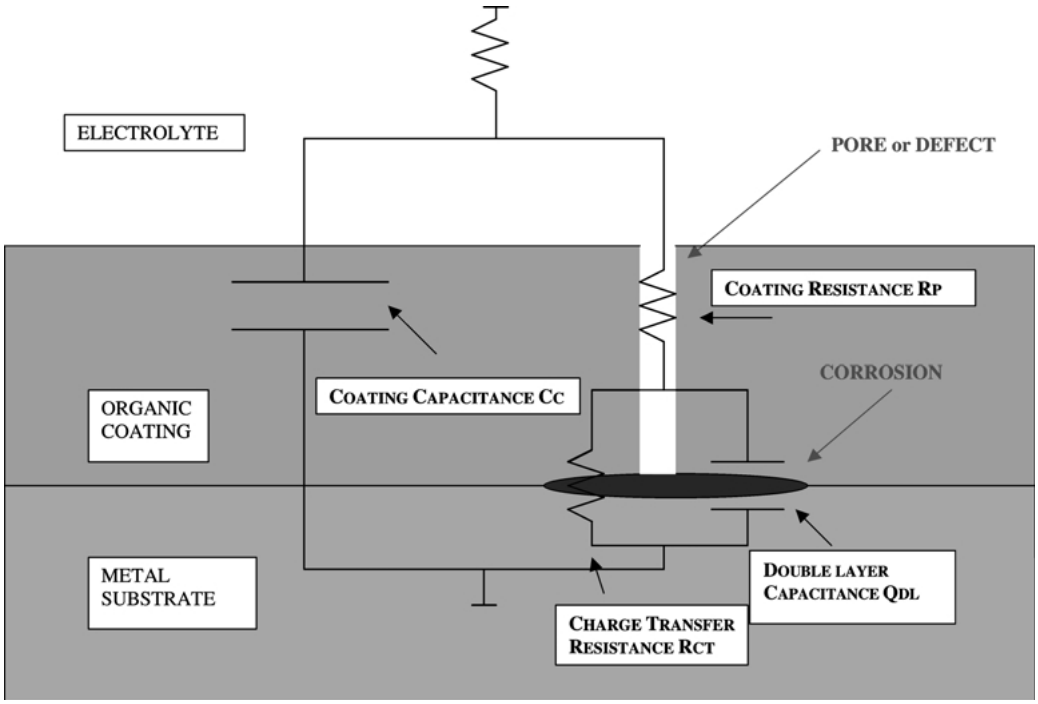

Fig. 1. Equivalent electrical circuit for an organic coating with a defect.

where R°_{ct} and C°_{dl} are the specific parameter values (per unit area), while A_r is the reactive area and A_w the wet area. Clearly we can assume A_w coincident with A_r and they are the same as A_p at the start of the test, when any delamination process, such as loss of adhesion of the coating from the substrate, can be considered negligible.

Equation 2 is more difficult to apply practically as it is not easy to measure the value of R°_{ct}, which is the specific charge transfer resistance at the bottom of the defect, not necessarily the same value measurable on exposed metals [14]. The electrochemical conditions inside the defect can differ, for example the oxygen concentration, affecting the corrosion rate. In contrast the C°_{dl} values depend less on the local physical-chemical conditions and are therefore easier to estimate; for this reason we prefer to use the latter parameter instead of R_{ct} for defect evaluation [13].

This experimental work consists in the application of the equations shown above to galvanized steel covered by organic coatings with artificial defects of known dimensions, verifying the reliability. The case of organic coatings on zinc is particularly critical and difficult due to the development of zinc corrosion products within defects leading to more complex EIS data analysis [15].

The final aim of the work, for which this paper is a first stage only, is to propose a procedure for estimating the total area of defects in industrial protective organic coatings.

2. Experimental details

Commercial protective coatings on phosphatized zinc electroplated steel (zinc coating thickness about 7 μm), based on PVDF (polyvinylidenfluoride resin) (thickness about 20 μm) were formed by a coil coating process.

From the same coil identical samples were cut and were observed by a stereomicroscope to identify any macrodefects (scratch, pinholes etc.) in the coating. We caused artificial defects in the samples by drilling with a very sharp steel tool (for dental use) down to the substrate. To avoid any substrate perforation, the drill was connected to an electrical instrument that stopped operation as soon as electrical contact between the tool and the substrate was established. We could produce defects with three diameters: 65, 100 and 200 μm. The defect morphology and dimensions were checked by scanning electron microscopy (SEM). The samples were then immersed in 0.3% Na_2SO_4 aerated solution.

The three-electrode electrochemical cell was obtained by placing a plastic cylinder on the sample sheet with the artificial defect at the centre and filling with the test solution. The exposed surface area was about 10 cm^2. A platinum counter electrode and an Ag/AgCl electrode as reference were used.

Impedance data were obtained on coated samples using a PAR 283 potentiostat and a Solartron 1255 frequency response analyser. The impedance measurements were carried out over a frequency range of 100 kHz to 100 mHz (5 frequencies per decade) using a 10 mV amplitude of sinusoidal voltage, in a Faraday cage to minimize external interference on the system. The impedance measurements were collected for about 1 h.

The impedance spectra were analysed using the fitting software Equivcrt by B. Boukamp.

3. Results and discussion

Figure 2 shows the typical morphology of an artificial defect with a diameter of 200 μm (Figure 2(a) front view and (b) cross section). A regular shape can be seen, which is, however, far from the ideal as used for the defect model, cylindrical. The defect appears more like a part of a cone and some accumulations of polymeric materials are visible close to the border of the defect. It is also possible that some zinc and polymer were spread at the bottom of the defect. However we assumed the quality of the defect to be satisfactory for our aims mainly because, despite the nonideal shape, such defects are easily reproducible, while any other way of producing small reproducible defects, for example by using electrical discharge and laser ablation, gave unsatisfactory results.

In the following discussion we consider the conical shape in the calculation of the average section of the defect and in the calculation of the area at the bottom of the defect (see Figure 2(b)).

Figure 3(a) shows the typical Nyquist plot obtained with the traditional cell. The data is very difficult to model using equivalent electrical circuits because during immersion corrosion products accumulate within the defect changing the impedance continuously as a consequence of an increasing diffusion contribution.

To minimize this problem we changed the cell configuration by rotating the samples of 180° to favour migration of corrosion products from the defect by gravity (new cell, Figure 4). The Nyquist diagram obtained in such a case is shown in Figure 3(b). The diagrams were obtained in both cases after about 5 h immersion in the solution with the same defect dimension (dia. 200 μm). In this case the data analysis with equivalent electrical circuits is easier, but in any case an element of the circuit related to a mass diffusion control (Warburg) is still present in series with the charge transfer resistance. After removing the samples from the electrolyte it was always possible to note the presence of dark corrosion products at the bottom of the defects. Moreover, we noted a few anomalous impedance results showing higher impedance; for these, despite the new configuration cell, we observed corrosion products physically blocked inside the defects. We suppose that the morphology of these defects (the presence of polymer residues) can favour accumulation of corrosion products even for a new cell. Here, the impedance is higher and therefore reproducibility of the EIS decreases and result dispersion increases.

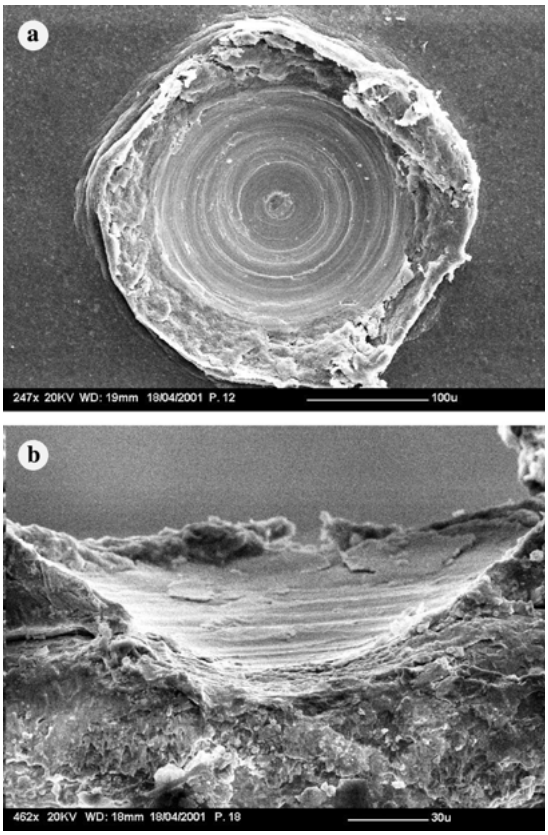

Fig. 2. Front view (a) and cross section (b) of a defect with 200 μm diameter.

In all measurements however the diffusion contribution partially overlaps the contribution to the impedance due to the coating and the contribution due to the electrochemical reactions at the bottom of the defect. Thus, accurate measurement of the parameters useful in determining the defect area (coating resistance, double layer capacitance) is very difficult. We tried to alter the measuring conditions by modifying the measurement potential. Instead of the open circuit potential, which is about -1050 mV vs Ag/AgCl, we measured the impedance at -1100 mV vs Ag/AgCl. This leads to about 50 mV of cathodic polarization for our system. This value is a compromise to be sure we can consider any anodic reaction as negligible, and therefore the production of corrosion products negligible, but also to maintain the cathodic reaction under activation control and to avoid diffusion control of the reaction due to oxygen diffusion. This condition was verified by measuring a cathodic polarization curve on the sample. A typical impedance plot, again measured after about 5 h immersion is shown in Figure 3(c). Under these conditions the impedance data analysis is easy and the results reproducible and, even if it is difficult to recognise by observing the diagram in Nyquist or in Bode representation, the impedance data are characterised by two time constants, as in Figure 3(a) and (b).

Comparing the diagrams in Figure 3 we can see that the impedance values of the samples measured at the free corrosion potential are comparable, slightly lower in the case of the new cell sample configuration because of the reduction of the presence of corrosion products, while a higher impedance was measured in the case of measurements of cathodic polarization.

The advantages of using cathodic potentials are also related to the fact that having not only zinc but also steel, in some cases at the bottom of the defect is not critical. It is impossible to avoid the drill reaching, in some cases, the steel under the zinc coatings. In general

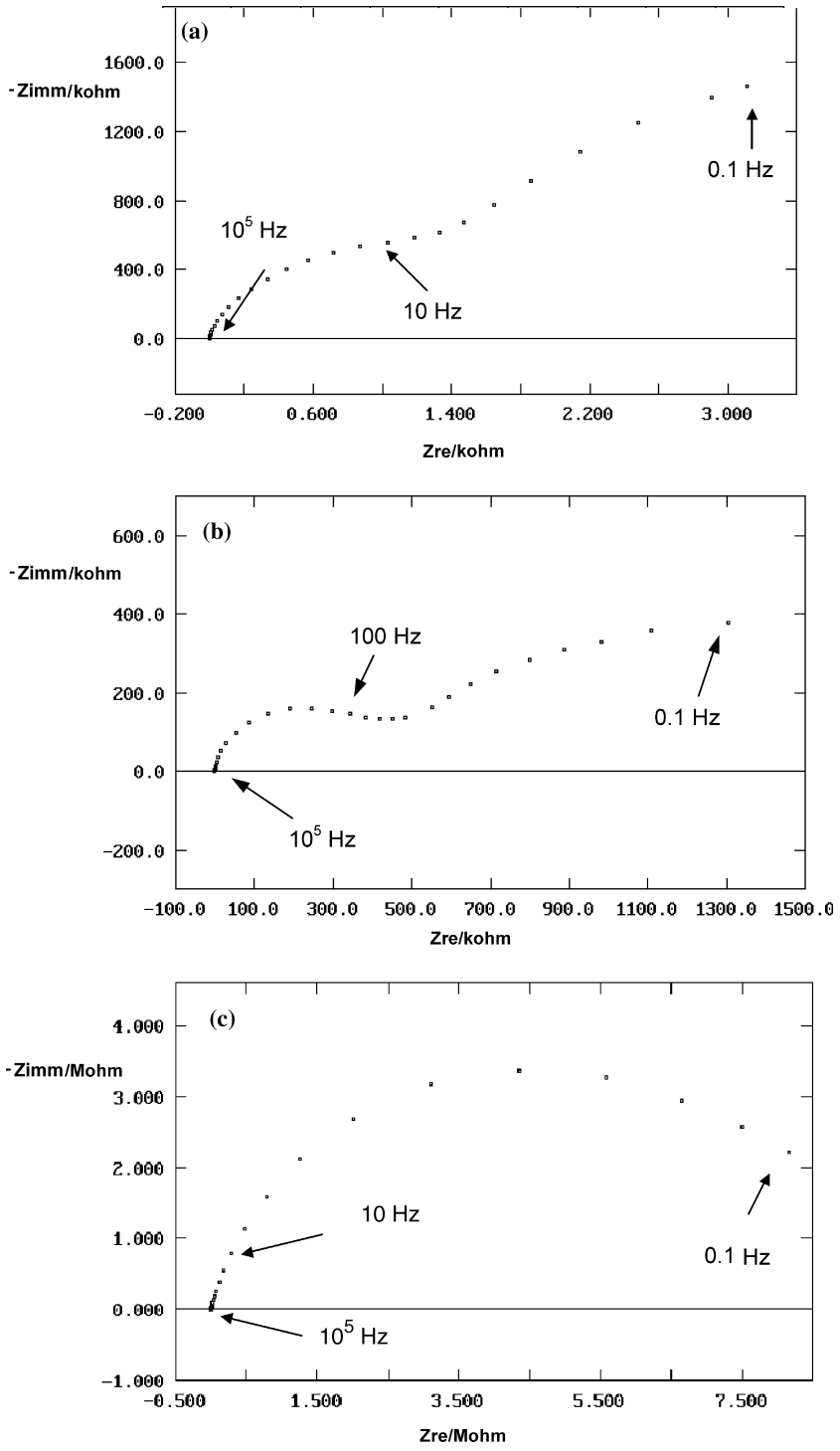

Fig. 3. Nyquist plots obtained after 5 h of immersion with samples with a defect of 200 μm diameter at free corrosion potential traditional cell (a), new cell (b) and new cell at −1100 mV vs Ag/AgCl (c).

we suppose that the defect surface is mainly zinc because we noted that the depth of the hole is less than the sum of the thickness of the organic coating and the zinc. Moreover, the free corrosion potential (−1060 mV vs Ag/AgCl) is typical for zinc and not for steel in the testing solution, but it is possible that some small areas of steel are in contact with the electrolyte. The anodic reaction (metal dissolution) of Zn and steel are very different as also are the chemical nature of the corrosion products. Enhancement of the corrosion reaction due to galvanic coupling could occur, but in the case of the cathodic reaction, steel and Zn catalyse the reaction in a similar way.

There are also disadvantages in using cathodic polarization. The main problem is that during the cathodic polarization some cathodic disbonding of the coating from the substrate may be promoted and, more generally, the sample conditions are modified. We suppose,

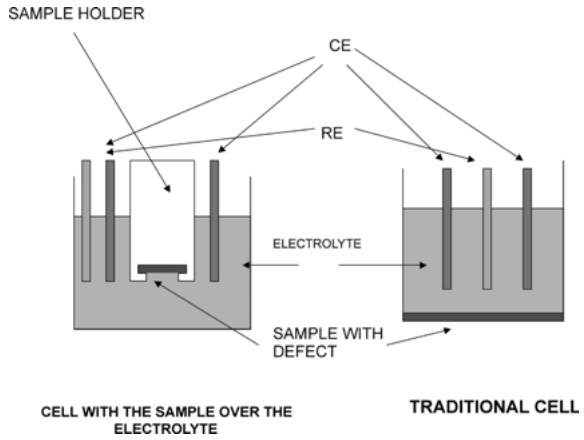

Fig. 4. Geometry of the new and traditional cell.

however, that in the short measuring time (about 1 h) the area changes are negligible if compared with the initial area of the artificial defects. Under these conditions we can use the model of Figure 1 to analyse the EIS data.

As previously discussed, the parameters of great interest for defect area determination are the coating resistance (R_p) and the parameters related to the bare metal surface: double layer capacitance, Q_{dl}, and charge transfer resistance, R_{ct}. Considering these last two parameters we decided to analyse in detail only the Q_{dl} values because, in principle, both should give the same results, but the R_{ct} values can change during the testing time thus changing the kinetics of the electrochemical reaction, while the specific Q_{dl} values (per unit of area) are more constant and more independent of the metal substrate (zinc or steel).

As an example, in Figure 5, we show the trend with immersion time of the double layer capacitance Q_{dl} for four equivalent samples with 200 μm diameter artificial defects. Good reproducibility of the electrochemical data is observed showing an increase in these values as a function of time. This trend may be due to the introduction of stress and deformation at the metal-coating interface during mechanical defect production, causing limited coating detachment. Limited, but measurable, cathodic disbanding phenomena increasing the metallic area in contact with the electrolyte may also occur. For this reason we decided to use the average value at the beginning of the test (a few minutes).

By similar means we obtained the Q_{dl} values for all the defect dimensions. The results as a function of the area dimension determined optically are shown in Figure 6. An interesting aspect of the plot is the linear correlation between double layer capacitance and defect dimension, as expected from Equation (3). However, we must consider that, due to the large testing area, some natural pores and defects could be present in the samples in addition to the artificial defect, thus modifying the values in Figure 6. For this reason we tested, under the same conditions, samples with no artificial defects and analysed the electrochemical data using the same equivalent electrical circuit. The Q_{dl} results are shown in Figure 7. From the figure, showing four duplicate samples, we can obtain a value of the double layer capacitance due to the presence of natural pores in the coating, as approximately 2.5 nF. We subtract this value from the data in Figure 6 to obtain the Q_{dl} values related only to the artificial defect. The results are in Figure 8 where we also show a point obtained with a double defect, two defects with a defect area close to the area of a larger single artificial defect.

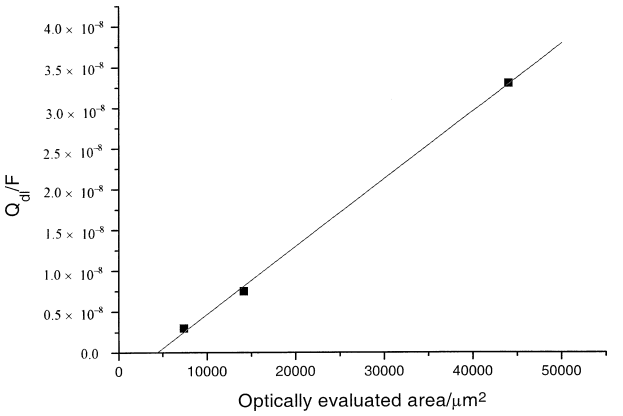

Fig. 6. Double layer capacitance (Q_{dl}) against optically evaluated area.

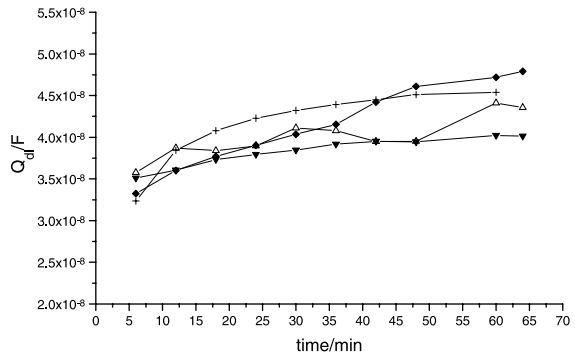

Fig. 5. Double layer capacitance (Q_{dl}) trend with immersion time for samples with 200 μm defect (four duplicated samples).

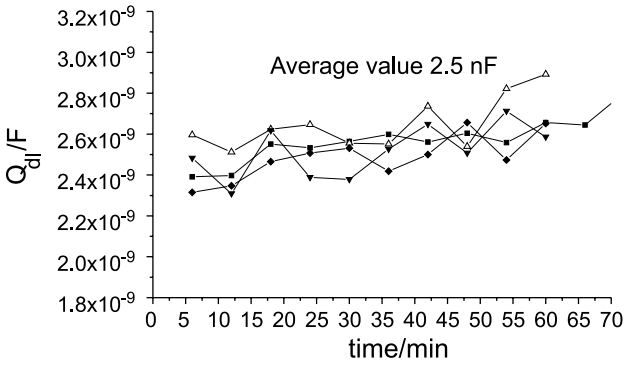

Fig. 7. Double layer capacitance (Q_{dl}) trend with the immersion time in the case of samples without artificial defect (four duplicated samples).

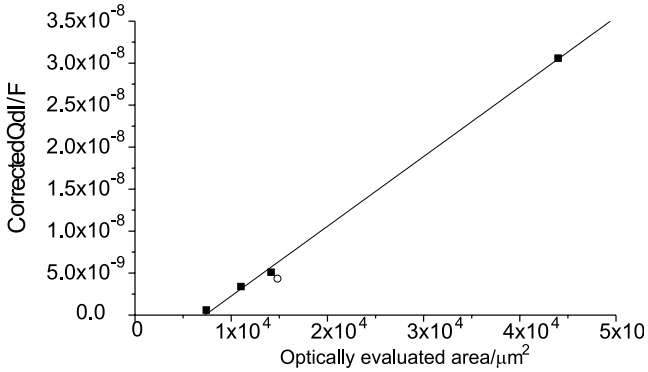

Fig. 8. Corrected double layer capacitance (Q_{dl}) against optically evaluated area. Key: (■) single defect, (◯) double defect.

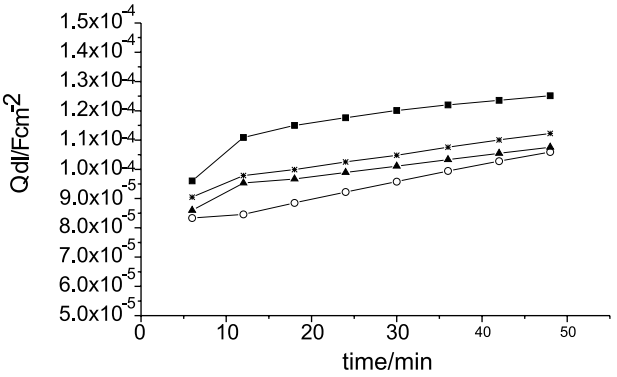

Fig. 10. Double layer capacitance (Q_{dl}) trend with immersion time for bare zinc in cathodic polarization conditions (−1100 mV vs Ag/AgCl) (four duplicated samples).

Here too, the trend shows a good linear correlation, but the line does not pass through the origin; in other words, if we extrapolate to an artificial defect area equal to zero, the double layer capacitance is not zero but negative. This strange result is, in our opinion, only due to measurement errors causing a contribution to the impedance, probably due to the cell configuration, which could be subtracted from the total impedance to obtain a more precise result.

By adding a constant, we can cause the line to pass through the origin and we see good correlation between the values of the defect area calculated from the Q_{dl} data and the results obtained optically, (Figure 9) by assuming a value for the specific double layer capacitance of the substrate of 83 μF cm^{-2}. This value, obtained by fitting to a line the results in Figure 9, is in good agreement with the experimental specific double layer capacitance measured on bare zinc in the same solution and shown in Figure 10 for four equivalent samples (Figure 10). It is interesting to note that the point in Figure 9 with the maximum error from the interpolation line is the point corresponding to the double defect. It is possible that, in this case, the error in the area evaluation by optical observation is higher. The coating resistance, R_p, as a function of the defect dimension is shown in Figure 11. The plot shows the data versus the inverse of the area as this representation should produce a straight line (Equation 1). However, it is evident from Figure 11 that the trend is nonlinear, the figure shows a parabolic relationship, for example, and therefore the assumption that the electrolyte resistivity ρ is constant is evidently wrong. It is possible that an electrical interaction exists between the charge carriers (ions) and the polymeric matrix of the coating. In this case the ionic

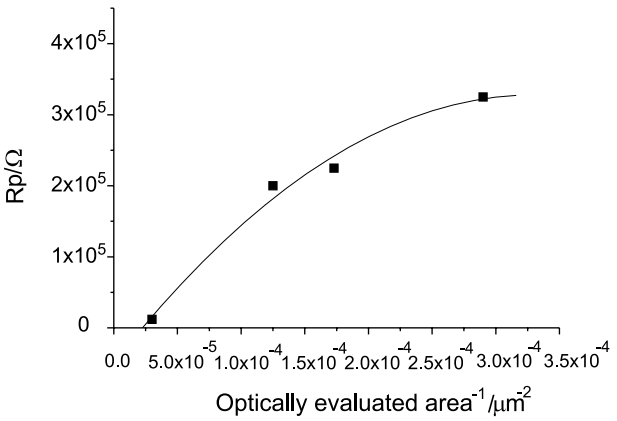

Fig. 11. Pore resistance R_p against optically evaluated area.

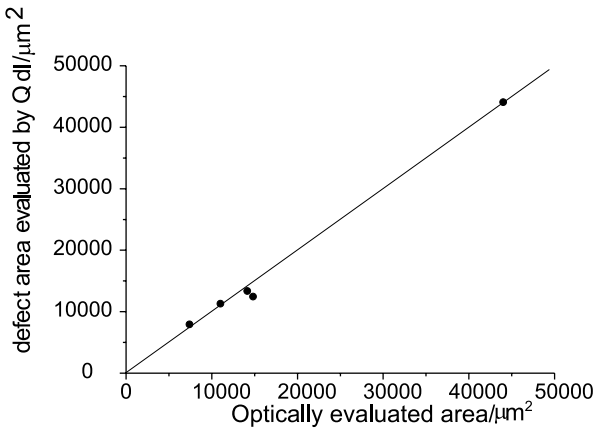

Fig. 9. Defect area evaluated by Q_{dl} against optically evaluated area.

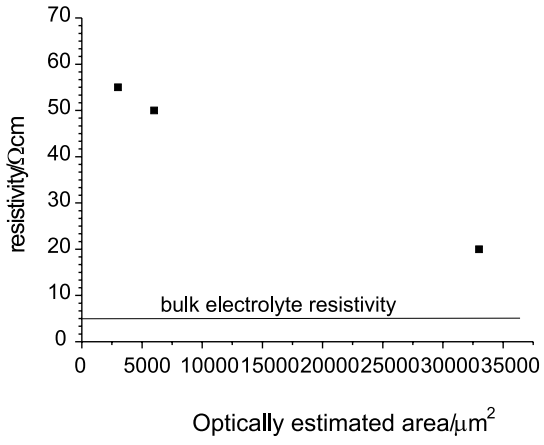

Fig. 12. Resistivity against optically evaluated area.

mobility should decrease and the electrolyte resistivity ρ increase by decreasing the defect dimension.

To appreciate this point, the value of the resistivity ρ as a function of the defect dimension measured optically is shown in Figure 12. The differences for smaller defects are not significant and within experimental error range. This is confirmed by the comparison of the average value in the case of small defects (about 50 Ω cm) and the value for 200 μm of diameter defects (about 20 Ω cm): increasing the defect dimension decreases the resistivity ρ towards the bulk electrolyte resistivity which is about 5 Ω cm.

4. Conclusions

Coil coated galvanized steel with small artificial defects was studied using electrochemical impedance spectroscopy to develop an experimental approach that can measure defect dimensions.

(i) To optimize the data acquisition and analysis on coated galvanized steel a specific cell geometry and EIS measurements under cathodic polarization (−1100 mV vs Ag/AgCl) were chosen.

(ii) In the experimental range of defect dimensions there is a linear relationship between the double layer capacitance Q_{dl} and the defect area. The value of the specific double layer capacitance obtained experimentally on bare zinc can be used to estimate the defect area in Equation 3.

(iii) The coating resistance R_p does not show a linear correlation with defect dimension, at least for large defect dimensions. The resistivity inside the defect is higher than the electrolyte resistivity and increases with reduction of the defect dimensions, demonstrating an electrical interaction between ions and the coating inside the defects.

Some aspects are still under discussion:

(iv) The linear correlation between Q_{dl} and defect area should be demonstrated for smaller defects, of diameter of the order of microns, to be useful for exposed area determination for coatings with natural defects.

(v) A general relationship between the pore or defect dimensions and the electrolyte resistivity inside defects has not yet been found

Acknowledgements

The authors acknowledge the assistance of Luca Benedetti and Andrea Tomasi in carrying out electrochemical measurements.

References

1. W. Funke, *in* A. Wilson, J. Nicholson and H. Prosser (Eds), 'Surface Coatings 1', (Elsevier, Oxford 1988).
2. J.H.W. DeWit, *in* P. Marcus and G. Oudar (Eds), 'Corrosion Mechanisms in Theory and Practice' (Marcel Dekker, New York, 1995).
3. H.R. Hamburg (Ed.), (Chapman & Hall, London, 1979). 'Hess's Paint Film Defects: their Cause and Cure'.
4. Z.W. Wicks, F.N. Jones and S.P. Pappas (Eds), (J. Wiley & Sons, New York, 1994) 'Organic Coatings Science and Technolgy'.
5. A. Amirudin and D. Thierry, *Prog. Org. Coat.* **26** (1995) 1.
6. P.L. Bonora, F. Deflorian and L. Fedrizzi, *Electrochim. Acta* **41** (1996) 1073.
7. F.M. Geenen, J.H.W. de Wit and E.P.M. van Westig, *Prog. Org. Coat.* **18** (1990) 299.
8. R. Hirayama and S. Haruyama, *Corrosion* **47** (1991) 952.
9. F. Deflorian, L. Fedrizzi, A. Locaspi and P.L. Bonora, *Electrochim. Acta* **38** (1993) 1945.
10. R.D. Armstrong, J.D. Wright and T.M. Handyside, *J. Appl. Electrochem.* **22** (1992) 795.
11. V. Lavaert, M. De Cock, M. Moors and E. Wettink, *Prog. Org. Coat.* **38** (2000) 213.
12. F. Deflorian and L. Fedrizzi, *J Adhes Sci Tecnol* **13** (1999) 629.
13. R.D. Armstrong and D. Wright, *Electrochim Acta* **38** (1993) 1799.
14. H. Leidheiser, *Corrosion* **39** (1983) 189.
15. A. Amirudin and D. Thierry, *Prog. Org. Coat.* **30** (1997) 109.